Monthly Notices
of the
ROYAL ASTRONOMICAL SOCIETY

MNRASL **433,** L54–L58 (2013)
Advance Access publication 2013 June 3

doi:10.1093/mnrasl/slt057

Measuring the slopes of mass profiles for dwarf spheroidals in triaxial cold dark matter potentials

Chervin F. P. Laporte,[1]⋆ Matthew G. Walker[2]† and Jorge Peñarrubia[3,4]

[1]*Max Planck Institute for Astrophysics, Karl-Schwarzschild-Strasse 1, D-85740 Garching, Germany*
[2]*Harvard–Smithsonian Center for Astrophysics, 60 Garden St, Cambridge, MA 02138, USA*
[3]*Institute for Astronomy, The University of Edinburgh, Royal Observatory, Blackford Hill, Edinburgh EH9 3HJ, UK*
[4]*Ramón y Cajal Fellow, Instituto de Astrofísica de Andalucia CSIC, Glorieta de la Astronomía, E-18008 Granada, Spain*

Accepted 2013 April 30. Received 2013 April 30; in original form 2013 March 3

ABSTRACT

We generate stellar distribution functions (DFs) in triaxial haloes in order to examine the reliability of slopes $\Gamma \equiv \Delta\log M/\Delta\log r$ inferred by applying mass estimators of the form $M \propto R_{\rm e}\sigma^2$ (i.e. assuming spherical symmetry, where $R_{\rm e}$ and σ are luminous effective radius and global velocity dispersion, respectively) to two stellar subpopulations independently tracing the same gravitational potential. The DFs take the form $f(E)$, are dynamically stable and are generated within triaxial potentials corresponding directly to subhaloes formed in cosmological dark-matter-only simulations of Milky Way and galaxy cluster haloes. Additionally, we consider the effect of different tracer number density profiles (cuspy and cored) on the inferred slopes of mass profiles. For the isotropic DFs considered here, we find that halo triaxiality tends to introduce an anticorrelation between $R_{\rm e}$ and σ when estimated for a variety of viewing angles. The net effect is a negligible contribution to the systematic error associated with the slope of the mass profile, which continues to be dominated by a bias towards greater overestimation of masses for more concentrated tracer populations. We demonstrate that simple mass estimates for two distinct tracer populations can give reliable lower limits for Γ, irrespective of the degree of triaxiality or shape of the tracer number density profile.

Key words: galaxies: kinematics and dynamics – galaxies: structure.

1 INTRODUCTION

The Milky Way's (MW) dwarf spheroidal (dSph) satellites include the most dark-matter-dominated galaxies known, with dynamical mass-to-light ratios ranging from of the order of $\sim$10 to several hundreds in solar units (Mateo 1998). This makes dSphs objects of prime interest for studying the distribution of dark matter in galaxies. dSphs lack atomic hydrogen; therefore, methods for measuring dSph masses must rely on the kinematics of their pressure-supported stellar populations. In the past decade, many techniques have been developed with the goal of determining the internal mass distributions of dSphs: spherical Jeans modelling (Łokas & Mamon 2001; Strigari et al. 2006; Koch et al. 2007; Battaglia et al. 2008; Walker et al. 2009; Wolf et al. 2010), phase-space modelling (Wilkinson et al. 2002; Amorisco & Evans 2011), the multiple stellar populations method (Walker & Peñarrubia 2011), the use of the virial theorem for spherical and flattened systems (Agnello & Evans 2012) as well as axisymmetric Jeans modelling (Hayashi & Chiba 2012) and Schwarzschild modelling (Breddels et al. 2012; Jardel & Gebhardt 2012).

Complicating most analyses is the fact that the inferred dynamical mass is degenerate with the anisotropy of the velocity dispersion tensor and the latter is poorly constrained by available line-of-sight velocity data. While this degeneracy leaves the full mass profile underconstrained in a standard Jeans analysis (Strigari et al. 2006; Walker et al. 2009), its relative weakness near the half-light radius of the stellar tracer makes estimates $M(R_{\rm e}) \propto \kappa R_{\rm e}\sigma^2$ (where $R_{\rm e}$ and σ are luminous effective radius and global velocity dispersion, respectively, and κ is a constant) robust to various forms of anisotropy and/or even to the shape of the mass profile (Walker et al. 2009; Wolf et al. 2010).

The presence of at least two chemodynamically distinct stellar subpopulations in several dSphs (Tolstoy et al. 2004; Battaglia et al. 2011) then provides a unique opportunity to measure the slopes of dSph mass profiles, $\Gamma \equiv \Delta\log M/\Delta\log r$, directly by estimating $M(R_{\rm e})$ at two different effective radii. Walker & Peñarrubia (2011, 'WP11' hereafter) introduce a statistical method that uses estimates of stellar positions, velocities and metallicities to estimate $R_{\rm e}$ and σ for each of two stellar subpopulations within the Fornax and Sculptor dSphs, obtaining $\Gamma = 2.61^{+0.43}_{-0.37}$ and $2.95^{+0.51}_{-0.39}$,

⋆ E-mail: cfpl2@mpa-garching.mpg.de
† Hubble Fellow.

respectively. Taken at face value, these measurements exclude, with significance ∼96 and ∼99 per cent, respectively, the Navarro, Frenk & White (1997, 'NFW' hereafter, $\Gamma \leq 2$ at all radii) profile that is often invoked to characterize density profiles of cold dark matter (CDM) haloes formed in dissipationless cosmological simulations. WP11 tested their method against spherical dynamical models with various degrees of anisotropy and found that mass estimators of the form $M(R_e) \propto R_e\sigma^2$ systematically overestimate the enclosed mass more strongly for tracers that are more deeply embedded (i.e. more concentrated) in their host haloes. This bias implies that slopes $\Gamma \equiv \log M/\Delta\log r$ tend to be systematically *underestimated*, such that WP11's claim of their quoted levels of NFW exclusion was conservative.

However, despite the assumption of spherical symmetry that is common to most dSph studies [exceptions include the axisymmetric Schwarzschild analyses of Jardel & Gebhardt (2012) and the flattened models considered by Agnello & Evans (2012)], the composite stellar populations of real dSphs are clearly not spherical. The MW's 'classical' dSph satellites have ellipticities in the range $0.1 \lesssim \epsilon \lesssim 0.6$ (Irwin & Hatzidimitriou 1995). Furthermore, haloes formed in CDM cosmological simulations tend to be triaxial (Allgood et al. 2006; Vera-Ciro et al. 2011). Therefore, insofar as CDM represents the null hypothesis regarding cosmological structure formation, the relevance of inferences drawn from spherically symmetric analyses depends critically on their robustness to axisymmetric and triaxial cases.

Here we test the slope measurements of WP11 for robustness against non-spherical symmetry. We exploit the fact that in a triaxial potential, the energy is an integral of the motion and thus we can construct isotropic stellar distribution functions (DFs) of the form $f(E)$ even within triaxial N-body dark matter haloes. We use the prescription presented by Laporte et al. (2013) to build stellar DFs with various degrees of concentration within cosmological CDM haloes produced in the Aquarius (Springel et al. 2008) and Phoenix (Gao et al. 2012) runs to cover a wide range of triaxiality parameters from MW- to cluster-type environments. Section 2 discusses the numerical simulations and method used to generate DFs. Section 3 describes our use of samples from these DFs (projected along various lines of sight) to examine systematic errors inherent to the WP11 method for various forms of the tracer number density profiles. We discuss results and conclude in Section 4.

2 NUMERICAL METHODS

2.1 Dark matter haloes

For the modelling of dSph dark matter haloes, we use the Aquarius simulations (see Springel et al. 2008 for details). This is a set of six high-resolution dark-matter-only simulations of the formation of MW mass dark matter haloes in ΛCDM. In the level-2 resolution the particle mass is $\sim 10^4\,M_\odot$ and the softening length is $\epsilon = 65$ pc comoving. We extract a number of dark matter haloes in the mass range 10^9–$10^{10}\,h^{-1}\,M_\odot$, where $h = 0.73$, using the subhalo finder SUBFIND (Springel et al. 2001). This is in the range of $M_{\rm vir}$ estimated by Peñarrubia, McConnachie & Navarro (2008) for the classical MW dSphs. The shapes of the Aquarius subhaloes have axis ratios which increase with radius and which are mildly triaxial with axis ratios $\langle b/a\rangle \sim 0.75$ and $\langle c/a\rangle \sim 0.6$ at 1 kpc (Vera-Ciro, private communication). We also complement our sample with subhaloes drawn from cluster simulations (Gao et al. 2012) to bracket the range of possible triaxiality parameters for subhaloes in CDM and rescaled masses by a factor of 1000.

2.2 Generating tracers

The weighting scheme used here was developed Laporte et al. (2013) and is a generalization of that of Bullock & Johnston (2005) to triaxial systems. For details see Laporte et al. (2013). In short, in order to generate a luminous stellar profile, we take each simulation particle of energy $E = \frac{1}{2}v^2 + \Phi$ to simultaneously represent dark matter and stars in different amounts through the weight function $\omega(E) = \frac{N_*(E)}{N(E)} = \frac{f_*(E)g(E)}{N(E)}$, where N is the differential energy distribution, g is the density of states and asterisks denote stellar quantities. One generates $f_*(E)$ through specifying the target number density profile $\nu = \nu(r)$ and using the Eddington formula with an additional approximation to deal with the multivalued behaviour of $\Phi = \Phi(r)$ with spherical radius. In this way, the method creates a stellar profile which retains contours of the flattening of the total potential.

Fig. 1 displays projected number densities and line-of-sight velocity dispersion profiles obtained by sampling random projections of DFs (for two different stellar number density profiles and different concentrations) calculated using the machinery described above.

WP11 originally tested their method using models in which stellar populations trace dark matter potentials characterized by generalized Hernquist (1990, see also Zhao 1996) profiles:

$$\nu_*(r) = \nu_0 \left(\frac{r}{R_e}\right)^{-\gamma_*} \left[1 + \left(\frac{r}{R_e}\right)^{\alpha_*}\right]^{(\gamma_*-\beta_*)/\alpha_*} \quad (1)$$

and

$$\rho_{\rm dm}(r) = \rho_0 \left(\frac{r}{r_{\rm dm}}\right)^{-\gamma_{\rm dm}} \left[1 + \left(\frac{r}{r_{\rm dm}}\right)^{\alpha_{\rm dm}}\right]^{(\gamma_{\rm dm}-\beta_{\rm dm})/\alpha_{\rm dm}}. \quad (2)$$

For the stellar number densities, WP11 considered Plummer profiles, $(\alpha_*, \beta_*, \gamma_*) = (2, 5, 0)$, which provide good fits to dSph surface brightness profiles (Irwin & Hatzidimitriou 1995; McConnachie & Irwin 2006) and have the virtue of depending on a single parameter, the projected half-light radius R_e. They also considered

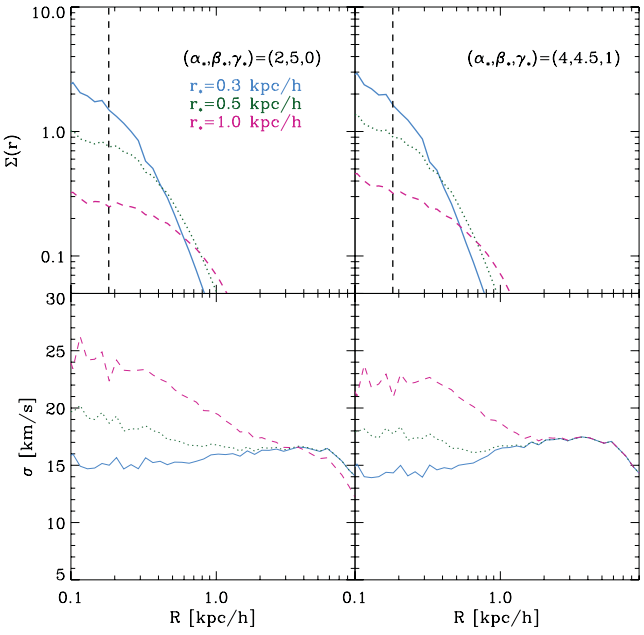

Figure 1. Projected number density and line-of-sight velocity dispersion profiles for one Aquarius subhalo using the present weighting scheme. Top left: Plummer profiles with $r_* = 0.3, 0.5, 1.0\,h^{-1}$ kpc. Top right: $(\alpha_*, \beta_*, \gamma_*) = (4, 4.5, 1)$ profiles with $r_* = 0.3, 0.5, 1.0\,h^{-1}$ kpc. The vertical dotted line marks the point where $r = 2.8\epsilon$.

alternative profiles that retain a luminous core ($\gamma_* = 0$) but fall off more slowly/quickly at large radius than do Plummer profiles,[1] with $(\alpha_*, \beta_*, \gamma_*) = (2, 4, 0)$ and $(2, 6, 0)$, respectively. Strigari, Frenk & White (2010) have shown that cuspy tracer number density profiles provide a good match to the observed surface brightness and velocity dispersion profiles of the composite stellar populations in dSphs. At a fixed half-light radius, a cuspy tracer component would have a lower velocity dispersion than would its cored counterpart. In order to test for sensitivity to the inner profile of the tracer components, here we consider models with stellar cusps $(\alpha_*, \beta_*, \gamma_*) = (4, 4.5, 1)$ as well as cored Plummer profiles with $(2, 5, 0)$.

3 MASS MODELLING: MULTICOMPONENT METHOD

The presence of multiple stellar populations in some dSphs enables the observer to estimate enclosed masses at two different half-light radii in the same potential. Testing their method on DFs drawn from spherically symmetric models with cored light profiles, WP11 find that masses tend to be overestimated more strongly for more concentrated stellar populations. As a result, the slope Γ tends to be underestimated, providing conservative lower limits on the true slope. We now use our models $f_*(E)$ to test whether this behaviour holds for the case of triaxial haloes and/or when the tracer number density profiles are cusped instead of cored.

3.1 The bias in the WP mass estimator: systematics

After calculating DFs as described above, we project each model along 100 random lines of sight uniformly sampled on a sphere. For each projection angle, we then calculate the half-light radius R_e of each population. In order to mimic the WP11 method, we estimate R_e by χ^2-fitting a Plummer profile to the tracers. The mass enclosed within R_e is then

$$M(R_e) \propto R_e \frac{\Sigma_{i=0}^{N} w_i (v_i - \bar{v})^2}{\Sigma_{i=0}^{N} w_i} \propto R_e \sigma^2, \quad (3)$$

where w_i are the N-body particle weights and σ is the global velocity dispersion of the tracers. The slope is then calculated as $\Gamma = \frac{\log(M_1/M_2)}{\log(r_1/r_2)}$.

In order to check whether the WP11 method continues to give conservative limits, Fig. 2 displays distributions of the bias $E[\Gamma] = \Gamma_{\rm est} - \Gamma_{\rm true}$ over all randomly chosen viewing angles. In nearly all cases the estimated slope is smaller than the true slope, such that the estimated slopes continue to represent conservative lower limits. This behaviour holds regardless of the degree of triaxiality and/or whether the light profile is cusped or cored.

Recently, Kowalczyk et al. (2013, 'K12' hereafter) have found that the use of a different mass estimator – one that refers to the velocity dispersion only of stars inside the half-light radius – would give less reliable limits on Γ, particularly when triaxiality is present. We confirm this result using our own DFs (Fig. 3): indeed, when velocity dispersions are estimated using only stars inside R_e of their respective subpopulation, the corresponding slope is less biased than that obtained from the WP11 estimator. As a result, slopes obtained from the K12 estimator are significantly more prone to overestimation (and thus unreliable exclusion limits for NFW profiles) –

[1] They actually considered models with $\gamma_* = 0.1$ because models with $\gamma = 0$ have $f(E) < 0$ in some regions. In the simulations the resolution limit already prevents this from happening for our models.

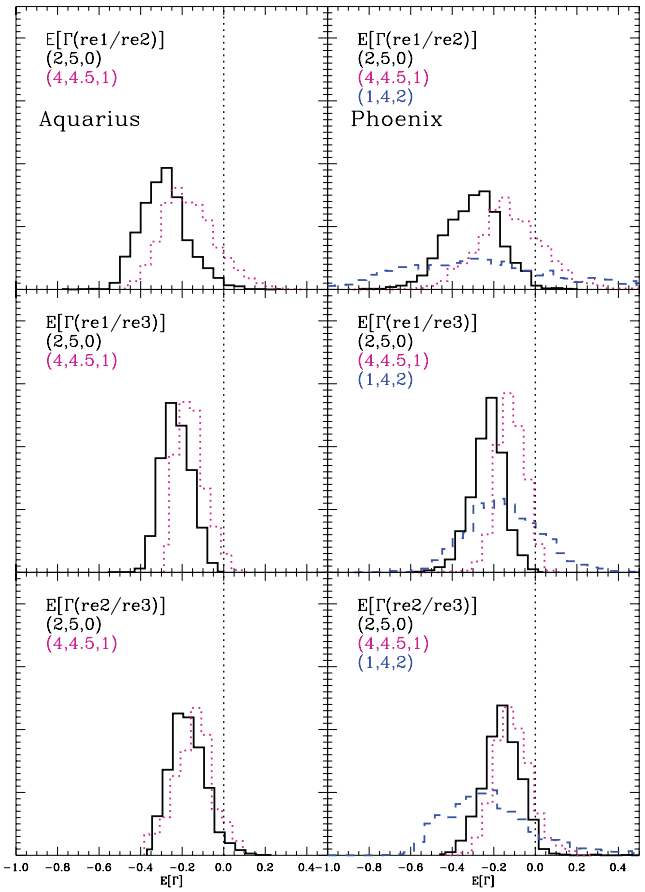

Figure 2. The stacked bias distribution in the slope determination of live N-body dark matter haloes (all observed through 100 different random lines of sight). The vertical line marks the point where $\Gamma_{\rm est} - \Gamma_{\rm true}$ is zero. Left-hand panels: results for Aquarius subhaloes for Plummer and (4, 4.5, 1) profiles (in black and dotted magenta, respectively). Right-hand panels: Phoenix rescaled subhaloes for Plummer, (4, 4.5, 1) and Jaffe profiles (in black, dotted magenta and dashed blue, respectively). The half-light radii of the stellar populations are determined through fitting a Plummer profile to the number density profile (as assumed in WP11). $(r_{e1}, r_{e2}, r_{e3}) = (0.3, 0.5, 1.0)\,h^{-1}$ kpc.

particularly for viewing angles along the morphological major axis – than are slopes obtained from the WP11 estimator.

In addition to stellar number densities used in studying dSphs, we also show results from additional tests for which we adopted the Jaffe profile, $(\alpha_*, \beta_*, \gamma_*) = (1, 4, 2)$, which can be used to model ellipticals and which has steep stellar cusp ($\gamma_* = 2$). In this case, we determine the half-light radius by fitting a de Vaucouleurs profile. For these cases with steep stellar cusps, we find that WP11's method becomes unreliable when the stellar populations are highly concentrated (top panel in Fig. 2); however, for sufficiently extended stellar populations the method still recovers a conservative (i.e. biased towards low values) estimate of the slope of the underlying mass profile, albeit with a more prominent tail towards positive values. While this is not a problem for dSphs which do not exhibit such strong stellar cusps, it should warn observers about the use of such an estimator for strongly cusped stellar tracer profiles.

3.2 Why triaxality does not matter so much?

We can understand the relative insensitivity of the WP11 method to triaxiality by considering the coupling of estimated quantities R_e

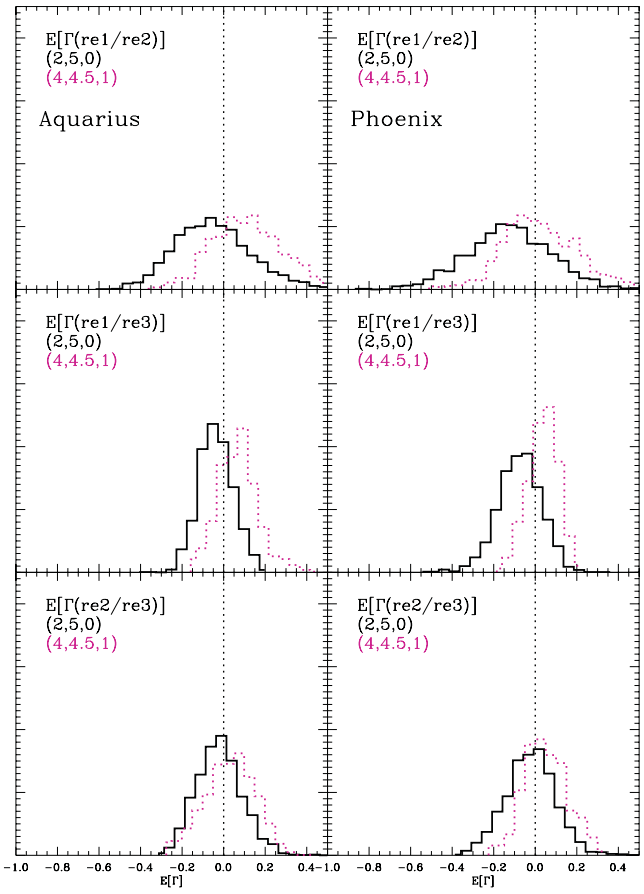

Figure 3. Same as Fig. 2 but showing results derived using the method used in K12. Clearly losing the kinematic information outside the half-light radius of the tracer makes the estimator highly unreliable. This method is not that used in WP11.

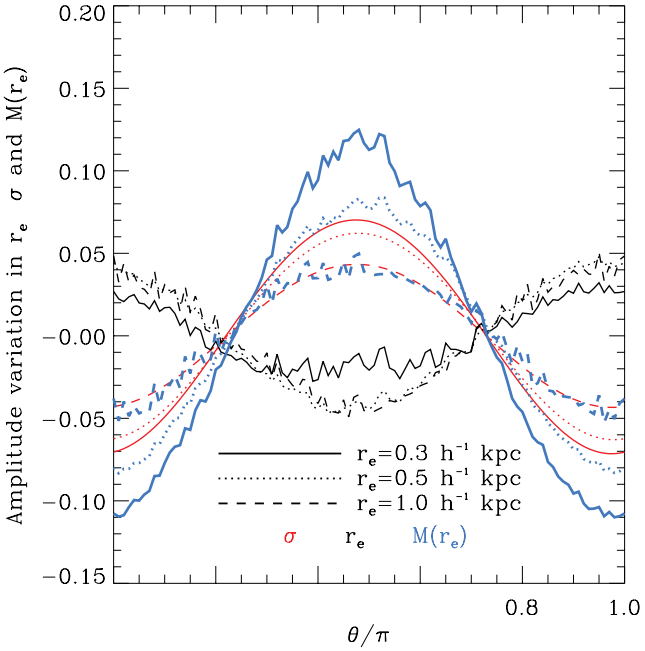

Figure 4. Amplitude of the variations in R_e (black), σ (red) and $M(R_e)$ (blue) for different stellar populations (different line styles) for an example halo from Aquarius as a function of angle θ, the polar angle in the plane of the major and minor axes of the halo evaluated at $1\,h^{-1}$ kpc. The anti-correlation in the behaviour of R_e and σ creates almost a cancellation and weak variations in $M(R_e)$. We also see that variations are greater the more embedded the stellar system similarly to the mass bias observed in WP11. This in turn explains why the slope estimates are still reliable under our $f(E)$ models in triaxial potentials.

and σ with respect to projection angle. Let us rotate an individual halo in the frame of its body axes (as evaluated at a radius of $1\,h^{-1}$ kpc) such that the major axis lies on the x-axis and the minor axis lies on the y-axis. We then observe it along different polar angles in the $x-y$ plane and estimate the half-light radius and velocity dispersion via the same χ^2-fitting procedure used above. We notice that when the velocity dispersion is large (along the major axis), the estimated value of R_e is at its minimum value and vice versa (Fig. 4). This anticorrelation of R_e and σ tends to cancel the effects of triaxiality on the mass estimator. Therefore, the slope Γ will be less sensitive because at a fixed angle θ any bias in $M(R_e)$ will cancel out in the estimate of Γ. This is why the biases we recover in Fig. 2 are similar to those found by WP11 for spherically symmetric models. The fluctuations in the mass estimates due to triaxiality vary from 10 to 20 per cent depending on the embeddedness of the tracer population.

4 DISCUSSION AND CONCLUSIONS

We have presented families of isotropic DFs of the form $f(E)$ in triaxial potentials extracted from dark-matter-only simulations. These span a range of dark matter density profiles for which we have tested the method of WP11. Our tests show that the method is generally able to place conservative limits on slopes of mass profiles, even when the light profiles have NFW-like cusps as advocated by Strigari et al. (2010). Thus, we conclude that triaxiality has little impact on published analyses of dSph stellar kinematics that assume spherical symmetry. The reason is that R_e and σ are anticorrelated over the range of projection angles, effectively cancelling the effects of triaxiality. However, we have found that the WP11 method can break down if the stellar tracers are highly concentrated and have steeply cusped number density profiles, e.g. the Jaffe profiles examined in Section 3.1. Some of the haloes which were identified by SUBFIND are strongly stripped and the tracer may not be entirely in equilibrium. However, using those models, we were still able to recover successful limits on the slope of the dark matter density profiles. This suggests that tidal stripping does not unduly impact the results of WP11.

Recently, a similar study on the same subject has been carried out by K12. Our work differs in three aspects.

(i) We consider haloes which form within a ΛCDM cosmological context. K12 have considered spherical models which get tidally stirred under a static potential.

(ii) Our models do not have rotation. Many galaxies in K12 still retain rotation, which is not observed in dSphs.

(iii) K12 do not test the robustness of WP11 to triaxality, but show that a mass estimator based on the velocity dispersion within the half-light radius of a tracer can misinterpret the true value of the slope of the total mass profile. We confirm their result in Fig. 3.

Finally, we note that given a density profile, there exist many possible velocity dispersion profiles which may be consistent with the observed data (allowing for anisotropy). However, WP11 showed that this is not an issue for their method under anisotropic Ossipkov–Merritt models but also those with constant anisotropy. Combined

with the results of our current study, the WP11 method seems to be robust to both anisotropy and halo triaxiality.

ACKNOWLEDGEMENTS

CFPL thanks Simon White for useful discussions, Mark Gieles and the IoA where early discussions began. MGW and JGP thank the MPA for its hospitality during their visit. The authors thank the Virgo Consortium for making their data available for this study. CFPL is supported by the Marie Curie Initial Training Network CosmoComp (PITN-GA-2009-238356). MGW is supported by NASA through Hubble Fellowship grant HST-HF-51283.01-A, awarded by the Space Telescope Science Institute, which is operated by the Association of Universities for Research in Astronomy, Inc., for NASA, under contract NAS5-26555.

REFERENCES

Agnello A., Evans N. W., 2012, ApJ, 754, L39
Allgood B., Flores R. A., Primack J. R., Kravtsov A. V., Wechsler R. H., Faltenbacher A., Bullock J. S., 2006, MNRAS, 367, 1781
Amorisco N. C., Evans N. W., 2011, MNRAS, 411, 2118
Battaglia G., Helmi A., Tolstoy E., Irwin M., Hill V., Jablonka P., 2008, ApJ, 681, L13
Battaglia G., Tolstoy E., Helmi A., Irwin M., Parisi P., Hill V., Jablonka P., 2011, MNRAS, 411, 1013
Breddels M. A., Helmi A., van den Bosch R. C. E., van de Ven G., Battaglia G., 2012, MNRAS, preprint (arXiv:1205.4712)
Bullock J. S., Johnston K. V., 2005, ApJ, 635, 931
Gao L., Navarro J. F., Frenk C. S., Jenkins A., Springel V., White S. D. M., 2012, MNRAS, 425, 2169
Hayashi K., Chiba M., 2012, ApJ, 755, 145
Hernquist L., 1990, ApJ, 356, 359
Irwin M., Hatzidimitriou D., 1995, MNRAS, 277, 1354
Jardel J. R., Gebhardt K., 2012, ApJ, 746, 89
Koch A., Wilkinson M. I., Kleyna J. T., Gilmore G. F., Grebel E. K., Mackey A. D., Evans N. W., Wyse R. F. G., 2007, ApJ, 657, 241
Kowalczyk K., Łokas E. L., Kazantzidis S., Mayer L., 2013, MNRAS, 431, 2796
Laporte C. F. P., White S. D. M., Naab T., Gao L., 2013, MNRAS, preprint (arXiv:1301.5319)
Łokas E. L., Mamon G. A., 2001, MNRAS, 321, 155
Mateo M. L., 1998, ARA&A, 36, 435
McConnachie A. W., Irwin M. J., 2006, MNRAS, 365, 1263
Navarro J. F., Frenk C. S., White S. D. M., 1997, ApJ, 490, 493 (NFW)
Peñarrubia J., McConnachie A. W., Navarro J. F., 2008, ApJ, 672, 904
Springel V., White S. D. M., Tormen G., Kauffmann G., 2001, MNRAS, 328, 726
Springel V. et al., 2008, MNRAS, 391, 1685
Strigari L. E., Bullock J. S., Kaplinghat M., Kravtsov A. V., Gnedin O. Y., Abazajian K., Klypin A. A., 2006, ApJ, 652, 306
Strigari L. E., Frenk C. S., White S. D. M., 2010, MNRAS, 408, 2364
Tolstoy E. et al., 2004, ApJ, 617, L119
Vera-Ciro C. A., Sales L. V., Helmi A., Frenk C. S., Navarro J. F., Springel V., Vogelsberger M., White S. D. M., 2011, MNRAS, 416, 1377
Walker M. G., Peñarrubia J., 2011, ApJ, 742, 20 (WP11)
Walker M. G., Mateo M., Olszewski E. W., Peñarrubia J., Wyn Evans N., Gilmore G., 2009, ApJ, 704, 1274
Wilkinson M. I., Kleyna J., Evans N. W., Gilmore G., 2002, MNRAS, 330, 778
Wolf J., Martinez G. D., Bullock J. S., Kaplinghat M., Geha M., Muñoz R. R., Simon J. D., Avedo F. F., 2010, MNRAS, 406, 1220
Zhao H., 1996, MNRAS, 278, 488

This paper has been typeset from a TEX/LATEX file prepared by the author.